

1
2
3
4 **Application of Artificial Neural Networks for Web-Post Shear Resistance of Cellular Steel**
5 **Beams**
6

7 Vireen Limbachiya ¹, Rabee Shamass ²

8
9 ^{1,2} Senior Lecturer in Civil Engineering, London South Bank University, School of Built
10 Environment and Architecture, London, UK

11
12
13
14 **Abstract**
15

16 The aim of this paper is to predict web-post buckling shear strength of cellular beams made
17 from normal strength steel using the Artificial Neural Networks (ANN). 304 developed
18 finite-element numerical models were used to train, validate and test 16 different ANN
19 models. To verify the accuracy of the ANN model, the ANN predictions were compared with
20 experimental and analytical results. Results show that ANN models that used geometric
21 parameters as an ANN input were able to predict web-post buckling strength to a higher level
22 of accuracy in comparison to models using only geometric ratios as an ANN input. An ANN-
23 based formula with 4 neurons was proposed in this study. In comparison to existing design
24 guidance, it is shown that an ANN model trained with the Levenberg-Marquardt
25 backpropagation algorithm is capable of predicting the web-post shear resistance to a higher
26 level of accuracy. The formula developed can be easily implemented in Excel or in user
27 graphical interface. It can be a potential tool for structural engineers who aim to accurately
28 estimate the web-post buckling of cellular steel beams without the use of costly resources
29 associated with FE analysis.
30

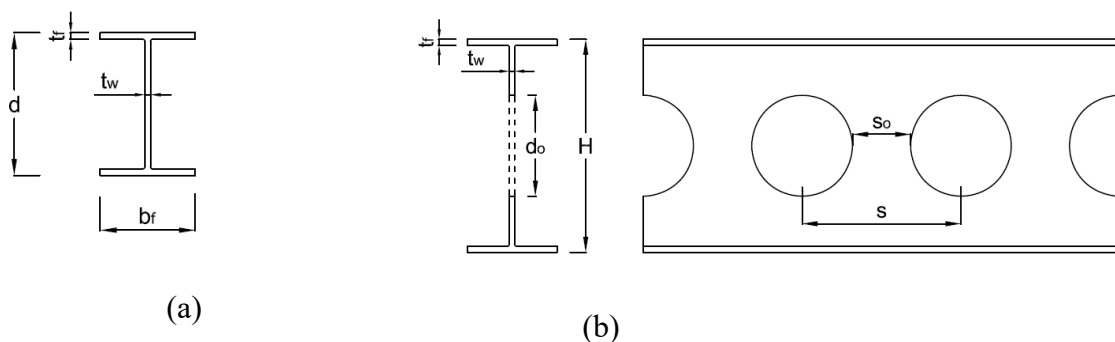
1. Introduction

33
34

35 Cellular beams are widely used to achieve long spans that allow for fewer columns and
36 footings in the structure, resulting in shorter construction times and cheap infrastructure costs
37 [1, 2]. They have been used for different structures that would benefit from open spaces such
38 as roofing with long spans, renovation, and strengthening and modernising historical
39 buildings while preserving their aesthetic design. Selecting cellular beams can reduce floor
40 zone depths as the services can be integrated with the floor beams which lower the building
41 height and cost.

42 Cellular beams can span much further than the regular I- beam sections since they have
43 higher depth-to-weight ratio, section modulus, and moment of inertia. They are usually
44 manufactured by cutting along the web of hot-rolled I-beam section in a certain pattern and
45 re-welding the upper and lower tees to form a cellular beam. Cellular beams will be named
46 all perforated beams with circular web opening.

47 Figure 1 shows parent I-beam and cellular beam sections. In this figure, H is the total height
48 of the cellular section; t_f and t_w are the flange and web thicknesses; b_f is the flange width; d is
49 the height of the parent section; d_o is the opening diameter; s and s_o are the centre-to-centre
50 spacing and edge-to-edge spacing of adjacent openings, respectively.



51

Figure 1: (a) Parent I-beam section; (b) Cellular beam geometry

52 The structural behaviour and type of failure of cellular beams are different from regular I-
53 beam sections. The failure modes of cellular beams observed experimentally are: global

54 bending failure (BF), Vierendeel bending failure (BF), lateral torsional buckling (LTB), web-
55 post rupture of weld joints, and web-post buckling (WPB), or lateral torsional buckling of
56 web-post due to high in-plane horizontal shear stress in the web-post. WPB consists of lateral
57 displacements of the web-post in double curvature accompanied by twisting deformations
58 [3], as can be observed in the Figure 2.



59

60 Figure 2. Web-post buckling mode of failure [4]

61 Many experimental tests have been conducted on cellular beams to investigate their structural
62 behaviour and failure modes [4-7]. It was observed from these experiments that the
63 dominated failure mode of cellular beams is the web-post buckling, particularly for
64 thin/narrow web-post cellular beams.

65 There are different approaches to predict the shear resistance of the web-post of cellular
66 beams. The design method by SCI publication 100 [8] was an early semi-empirical design
67 method for the WPB which proposed a relationship between maximum allowable web- post
68 moment and the web-post geometries. Grilio et al [4] proposed resistance curves to determine
69 the shear resistance in cellular beams for the web-post buckling. Lawson et al [9] suggested
70 another design approach to obtain the shear resistance of web-post based on the design of
71 strut analogy acting diagonally in the web-post. This method was adopted by SCI publication
72 355 [10] for WPB of cellular beams with large opening. More recently, Shamass and
73 Guarracino [11] proposed a new design model obtained from a simplified mechanical
74 approach for WPB which is based on the elementary model of an ideal inclined compressed

75 strut. This model can adjust the width, inclination and boundary conditions of the compressed
76 ideal strut to the geometry of the cellular beam and is applicable for normal and high strength
77 steel.

78 However, plastic buckling of structures remains a rather complicated problem depending on a
79 number of factors, as recently shown by investigations of one of the present authors [12-15]
80 and for such a reason the recourse to artificial intelligence methods, such as neural networks
81 and fuzzy logic (FL) may turn beneficial to these kinds of problems.

82 In fact, over the years, the application of modelling methods based on neural networks and
83 fuzzy logic (FL) have been implemented to solve various engineering problems. Artificial
84 Neural Networks (ANN) solve complex problems with the help of interconnected computer
85 elements and consist of 3 layers (input, hidden and output). The inputs in this case are the
86 geometric variables within a cellular steel section shown in Figure 1. The hidden layer
87 consists of neurons which recognises patterns and computes values from the input which in
88 turn predicts the response variable. Fuzzy control theory needs only to set a simple
89 controlling method based on engineering experience. Therefore, it is particularly useful in
90 complicated structural control system [16]. When comparing the two forms of modelling,
91 both provided great levels of accuracy, however, it has been concluded that ANN provides
92 better statistical results in comparison to FL [16-17].

93 ANN has been used to predict various forms of structural behaviour in steel elements such as
94 I-beams [18], composite columns [19], frames [20], welded flange plate steel connections
95 [21] and unstiffened steel plates [22], with some studies focusing on cellular and castellated
96 steel beam [23-29]. It was reported that ANN showed more accurate ultimate moment
97 capacities of castellated steel beams under lateral-distortional buckling (LTB) than those
98 predicted by current design rules such as EC3 and AISC, the later provided unsafe and
99 unconservative predictions [23]. In another study it was concluded that ANN-based formula

100 model trained on 140 castellated beams modelled using finite-element (FE) and Levenberg-
101 Marquardt algorithm provided accurate web-post buckling strength of castellated beams [29].
102 Sharifi et al. [26] used 96 data-based verified simulation to train ANN that predicted the
103 strength capacity of cellular beams under LTB. They reported that ANN gave reliable
104 estimations of the LTB strength capacity of steel cellular beams. Sharifi et al [25] trained an
105 ANN network with a database of 99 cellular steel beams which were loaded under two
106 concentrated loads and failed in LTB mode. The study compared 9 training algorithms in
107 MATLAB and found that the Levenberg-Marquardt algorithm provided the most accurate
108 predictions when reviewing the mean-squared error of the predicted results from the
109 considered training algorithms. Abambres et al [27] proposed ANN-based formula to predict
110 elastic buckling load of cellular beams subjected to distributed load. It was concluded that the
111 ANN-based formula yielded accurate predictions. Overall, studies showed that ANN is able
112 to provide fast results with the high level of accuracy when compared to experimental and
113 numerical results.

114 In this context, it can be noted that there is currently no research that aims at predicting the
115 web-post buckling of cellular beams using ANN. Therefore, the scope of this paper is to
116 predict the vertical shear strength of cellular beams made from normal strength steel S355
117 using ANN and to propose an ANN-based formula to accurately compute the web-post
118 buckling strength, in terms of independent geometrical parameters. The study makes use of
119 the FE model developed by Shamass and Guarracino [11] to generate the data that is
120 successively employed to train the ANN. The output of the ANN is then compared to
121 experimental data and current analytical analysis, with satisfactory results.

122

123

124

2. Development and validation of the numerical models

Full beam models are generally used for numerical validation and to investigate the structural behaviour of cellular elements. The single web-post models are widely used in the literature to investigate numerically the effect of geometric properties of the cellular beams on the shear resistance of the web-post [4, 5, 7]. In this study, both the full beam and the single web-post models are developed and validated.

Shamass and Guarracino [11] previously developed finite-element (FE) model using ABAQUS software for simply supported cellular beams subjected to a point load. The same FE model is used in this study since it has proven capable of providing a good prediction of the behaviour of steel cellular beams in terms of vertical shear resistance, load-displacement response and WPB failure. The steel cellular beams test results conducted by Grilo et al. [4] and Tsavdaridis and D’Mello [5] were used for the validation of the both full beam and the single web-post numerical models since all the cellular beams in these tests failed by pure WPB. The material was modelled using a multi-linear stress-strain relationship, including strain hardening. The cellular beam section and stiffeners were modelled using a general-purpose three-dimensional reduced integration shell element named S4R in ABAQUS.

Simply supported boundary conditions were used in the beams and loading was applied on the top flange of the beams under displacement control. A linear buckling analysis was first performed, followed by a nonlinear analysis using the Newton-Raphson solution method. Geometric imperfections were considered in the numerical model.

The single web-post model used in this study shares the same numerical considerations of the full beam model with respect to the type of element, material properties and initial imperfection. The boundary conditions and the load application of the web-post model are described in Grilo et al. [4] and shown in Figure 3.

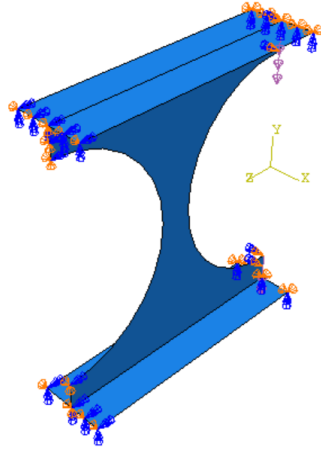


Figure 3: Single web-post model

149

150

151

152 Table 1 shows comparisons between the buckling shear loads observed experimentally (V_{Test})
153 by Grilo et al. [4] and Tsavdaridis and D’Mello [5] with those obtained numerically (V_{FE}) for
154 both the full beam and single web-post models. It can be observed that the buckling shear
155 loads from the single web-post model tend to be more conservative in comparison to those
156 from the full beam model. Grilo et al. [4] conducted numerical models for full beam, single
157 web-post and long beam models and found that long beam models predicted shear buckling
158 results close to those predicted by the single web-post models, since the long beam models
159 were less sensitive to border effects. Therefore, the single web-post models were not
160 influenced by the border effect. In summary, the validation of the single web-post model
161 confirms that the model can reasonably be utilised for further parametric study to predict
162 buckling shear load of WPB with minimum computational effort.

163

164

165

166

Table 1: Comparison between experimental and numerical vertical shear buckling load

Specimen	Buckling shear strength (V) (kN)			Percentage difference (%)	
	Test (V _{Test})	Numerical model (V _{FE})			
		Full beam	Single web- post	Full beam/test	Single web- post/test
A1	38	40.0	37.1	5.26	-2.3
A2	61.9	59.2	58.2	-4.34	-6.0
A3	70.7	65.6	65.2	-7.21	-7.8
A5	99.1	98.4	71.9	-0.75	-27.4
A6	102.2	102.5	96.7	0.26	-5.4
B1	54	54.9	53.1	1.57	-1.6
B2	79	75.6	78.9	-4.32	-0.2
B5	138.5	134.5	110.0	-2.91	-20.6
B6	150	148.6	137.7	-0.93	-8.2
C1	144.35	147.7	147.7	2.35	2.3
C2	127.5	120.0	101.4	-5.88	-20.5

168

169 3. Parametric study

170 In this section, the single web-post model described in the Section 2 is used to predict the
 171 shear buckling loads. The numerical shear buckling loads will then be used to train the
 172 artificial neural network models.

173 The steel grade is S355 with, elastic modulus E, yield stress f_y , ultimate stress f_u , strain at the
 174 onset of hardening ϵ_{st} and ultimate strain ϵ_u equal to 210 Gpa, 355 Mpa, 510 Mpa, 2.5% and
 175 18 %, respectively. The imperfection size is taken as H/500 [7].

176 The parameters characterising the web-post geometries resulting from the cutting process of
 177 the rolled I-beam are [8]:

$$e = \frac{d_o}{2} - \sqrt{\left(\frac{d_o}{2}\right)^2 - \left(\frac{s - d_o}{2}\right)^2} \quad (1)$$

$$H = d + \frac{d_o}{2} - e \quad (2)$$

$$s_o = s - d_o \quad (3)$$

178 In this study rolled sections presented in the Table 2 are used as the parent I-beam sections
 179 with slenderness ratios d/t_w range from 34.56 to 62.19. The opening ratio d_o/d is taken
 180 equal to 0.8, 0.9, 1, 1.1, and 1.2 and the spacing ratio s/d_o is taken equal to 1.1, 1.2, 1.3, 1.4,
 181 and 1.5.

182

183 Table 2: Parent I-beam sections used in this study

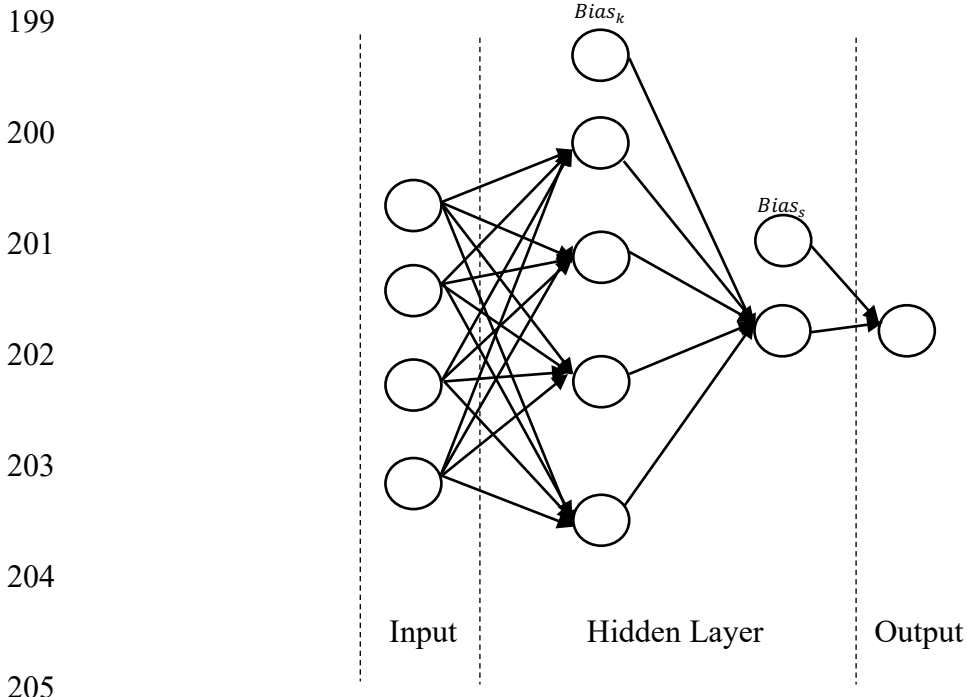
Section UB	152×89×16	203×102×25	245×102×28	254×146×37	305×102×28
d/t_w	33.91	35.65	41.33	40.63	51.45
Section UB	305×127×48	356×171×45	406×140×39	406×178×60	457×191×67
d/t_w	34.56	50.2	62.19	51.44	53.34
Section UB	457×191×74	457×152×82	533×165×85	610×178×100	
d/t_w	50.78	46.47	51.93	53.75	

184

185 4. Artificial neural network

186 4.1 Neural Network Architecture

187 The network architecture used in this paper is a Multi-Layer Perceptron Network
 188 (MLPN). The neural network toolbox with MATLAB [30] solves an input-output fitting
 189 problem with a two-layer feedforward neural network. Two-layer feed-forward network can
 190 fit multi-dimensional mapping problems arbitrarily well, given consistent data and enough
 191 neurons are provided to its hidden layer. It has been shown that the number of neurons within
 192 the hidden layer have an impact on the accuracy of the output. Figure 4 illustrates an example
 193 of 4 neurons ANN structure consisting of 4 input parameters and 1 output parameter.
 194 Each input parameter layer links with every neuron in the hidden layer and subsequently the
 195 neurons in the hidden layer links with the output layer. Each link is assigned with a synaptic
 196 weight (real number) which is dependent on the analysis of the training and validation data
 197 sets. $Bias_k$ and $Bias_s$ in Figure 4 are constant values that are added at the hidden layer and
 198 output, respectively.



206 Figure 4: ANN Model with 4 neurons in the hidden layer

207 **4.2 Input and Output Normalisation**

208 The progress of training can be reduced if training data defines a region that is relatively
 209 narrow in some dimensions and elongated in others [27]. Therefore, normalisation for
 210 variables across all data patterns should be implemented to improve the training process. In
 211 order to normalize the input and output parameters, Equation 4 was applied to all input and
 212 target parameters.

213

$$Y = \frac{(Y_{\max} - Y_{\min})(X - X_{\min})}{(X_{\max} - X_{\min}) + Y_{\min}} \quad (4)$$

214

215 Where Y_{\min} is the minimum value for each row of Y (default is -1), Y_{\max} is the maximum
 216 value for each row of Y (default is $+1$), X_{\max} is the maximum value of the input/target output

217 parameter, X_{\min} is the minimum value of the input/target output parameter, X is the actual
218 value and Y is the normalised value

219

220 **4.3 Learning Algorithm**

221 The synaptic weight and bias are network unknown parameters that are identified through the
222 learning. The ANN learning consists of training, validation and testing. The data points are
223 randomly grouped into training set, validation set and testing set, with 15%,15% and 70% of
224 the data being assigned respectively. While the training set is used to compute the gradient
225 and update the weights and biases, a process of cross validation takes place using the
226 validation data set so the generalization performance of the network can be verified. When
227 the optimum network parameters are defined, the test set will be used to assess the module
228 accuracy. The Levenberg-Marquardt back propagation training algorithm is adopted in this
229 study due to the high level of accuracy noted in previous studies [23-27] and it is suitable for
230 training small- and medium-sized problems. Golafshani et al. [31] stated that the back-
231 propagation algorithm involves two phases. The first one is the forward phase where the
232 activations are propagated from the input to the output layer. The second one is the backward
233 phase where the error between the observed actual value and the desired nominal value in the
234 output layer is propagated backwards in order to modify the weights and bias values.

235 **4.4 Setting up Artificial Neural Network**

236 In total, 304 input and output parameters were obtained from the numerical FE models to
237 produce the ANN. Equation 4 was applied to all input and output parameters and Table 3
238 provides the values required in order to normalise and de-normalise the inputs and outputs.

239

240

241

Table 3: Parameters used to normalise input and target values

<i>Input/Target Parameter</i>	Y_{\max}	Y_{\min}	X_{\min}	X_{\max}
H	1	-1	205.19	970.01
d_o	1	-1	121.92	728.88
s	1	-1	146.30	947.54
t_w	1	-1	4.5	11.3
d	1	-1	152.4	607.4
d_o/t_w	1	-1	19.06	505.89
H/d_o	1	-1	27.09	74.63
s/d_o	1	-1	1.27	1.75
d/d_o	1	-1	1.10	1.50
V	1	-1	19.06	505.89

242

243 Table 4 provides the details of the 16 models that were developed and analysed in this study.

244 For each of the input parameters reviewed, ANN models with 4, 6, 8 and 10 neurons in the
 245 hidden layer were created and analysed.

246 Table 4: Parameters of 16 ANN models produced

Model	Input parameters	Number of neurons in hidden layer				Output parameter
1	H, d_o , t_w , s, d	4	6	8	10	V
2	H, d_o , t_w , s	4	6	8	10	V
3	d_o/t_w , H/d_o , s/d_o	4	6	8	10	V
4	d_o/t_w , H/d_o , s/d_o , d/d_o	4	6	8	10	V

247

248 Equations 5 and 6 show the calculations which includes the transfer function that is required
 249 in order to determine the normalised output value based on the inputs provided [32].

$$O_s = \text{Bias}_s + \sum_{k=1}^r w_{k,l}^{ho} \cdot \frac{2}{(1 + e^{(-2H_k)}) - 1} \tag{5}$$

$$H_k = \text{Bias}_k + \sum_{j=1}^q w_{j,k}^{ih} \cdot I_j \quad (6)$$

250 Where, O_s represents the normalised output value, q is the number of input parameters; r is
 251 the number of hidden neurons; s is the number of output parameters; Bias_s and Bias_k are the
 252 biases of s^{th} output neuron and k^{th} hidden neuron (H_k), respectively; $w_{j,k}^{ih}$ is the weights of the
 253 connection between I_j and H_k ; $w_{k,l}^{ho}$ are the weights of the connection between H_k and O_l .

254

255 **4.5 Assessing Accuracy of Neural Network Output**

256 To assess the accuracy of the output the regression (R^2), Root Mean Square Error (RMSE)
 257 and Mean Absolute Error (MAE) were calculated using Equations 7, 8 and 9 respectively.

258

$$R^2 = 1 - \left(\frac{\sum_{i=1}^N (O_i - t_i)^2}{\sum_{i=1}^N (O_i)^2} \right) \quad (7)$$

$$\text{RMSE} = \sqrt{\frac{\sum_{i=1}^N (O_i - t_i)^2}{N}} \quad (8)$$

$$\text{MAE} = \frac{1}{N} \sum_{i=1}^N |O_i - t_i| \quad (9)$$

259 Where t_i and O_i are the actual and predicted shear resistance of the web-post of cellular beam,
 260 and N is the total number of data points in each set of data.

261

262 **4.6 Impact of Individual Input**

263 The weight from the input node to the hidden layer plays a crucial role in understanding the
 264 importance of the input parameters. An input value with a high positive weight will indicate
 265 that the input parameter has a significant impact on increasing the value of the output. If the
 266 weight of an input result is close to zero then this has minimal effect on the output. Similarly,

267 an input value with negative weight will indicate that increasing this value will decrease the
268 output value. In order to calculate the importance of each weight the Connection Weight
269 Approach was adopted. There are many approaches that can be used, and it was concluded
270 that the Connection Weight Approach provides the best method for accurately quantifying
271 variable importance [33]. It is important to note that this approach does not assess the
272 accuracy of the ANN model created using MATLAB, as it simply quantifies the
273 contributions of the predictor variables in the network. It provides a form of validation to the
274 model, as it can be used to compare with what would be expected to occur if there was to be
275 variation in a given input parameter. The Connection Weight Approach uses raw connection
276 weights, which accounts for the direction of the input–hidden–output relationship and results
277 in the correct identification of variable contribution [33]. Equation 10 shows the calculation
278 required to determine the impact of each input parameter based on the Connection Weight
279 Approach [33]. In this equation, the $Input_x$ represents the importance, XY represents the
280 input-hidden connection weights and $Hidden$ represents the hidden-output connection
281 weights.

$$Input_x = \sum_{Y=A}^E Hidden_{XY} \quad (10)$$

282 5. Results and discussion

283

284 5.1 ANN predictions

285

286 Table 5 provides the regression values for the training, validation and testing data sets. Table
287 6 provides the overall statistics for the 16 ANN models when applying Levenberg-Marquardt
288 backpropagation algorithm. Figures 5 and 6 are examples of the actual against predicted V
289 for models 1 and 2 with 4 neurons, respectively. Results from the Table 6 clearly show that
290 the ANN models consisting of individual geometric input parameters provides more accurate

291 predictions than the ANN models using geometric ratios only. The highest accuracy with
 292 geometric ratios is found for model 4 with 10 neurons for which the corresponding regression
 293 value is 0.7355. Although a regression value of 0.7355 shows some form of accuracy, the
 294 MAE and RMSE values mean that it is unsuitable to predict the shear resistance with high
 295 degree of accuracy. When reviewing models 1 and 2 which only take into consideration the
 296 input geometric parameters of the cellular beam (without geometric ratios), model 1 and
 297 model 2 with 8 and 10 neurons, respectively, provide the highest accuracy among the other
 298 ANN models. In conclusion, the ANN model 1 and model 2 predict the shear resistance of
 299 the web-post of cellular beam with high level of accuracy.

300 Table 5: Regression values for training, validation and testing data sets

MODEL	INPUT PARAMETERS	NO. OF NEURONS	R ²		
			Training	Validation	Testing
1	H, d _o , t _w , s, d	4	0.9945	0.9964	0.9950
		6	0.9989	0.9984	0.9990
		8	0.9997	0.9996	0.9995
		10	0.9996	0.9993	0.9991
2	H, d _o , t _w , s	4	0.9981	0.9977	0.9972
		6	0.9985	0.9979	0.9978
		8	0.9985	0.9987	0.9991
		10	0.9998	0.9995	0.9992
3	d _o /t _w , H/d _o , s/d _o	4	0.7671	0.8109	0.7711
		6	0.8493	0.8666	0.7759
		8	0.8541	0.8482	0.7712
		10	0.7037	0.7696	0.7068
4	d _o /t _w , H/d _o , s/d _o , d/d _o	4	0.7109	0.7014	0.7015
		6	0.8376	0.8279	0.8269
		8	0.8351	0.8365	0.7879
		10	0.8741	0.8233	0.8173

301
 302
 303
 304
 305
 306
 307
 308
 309
 310

311
312

Table 6: Output of ANN models

MODEL	INPUT PARAMETERS	NO. OF NEURONS	R ²	MAE	RMSE
1	H, d _o , t _w , s, d	4	0.9953	5.49	7.08
		6	0.9977	3.32	5.00
		8	0.9992	2.09	2.86
		10	0.9989	2.24	3.36
2	H, d _o , t _w , s	4	0.9959	5.03	6.67
		6	0.9967	4.5	5.94
		8	0.9973	4.01	5.49
		10	0.9993	1.81	2.76
3	d _o /t _w , H/d _o , s/d _o	4	0.6015	52.27	65.16
		6	0.7064	44.00	55.9
		8	0.7012	45.72	56.66
		10	0.5088	55.97	72.5
4	d _o /t _w , H/d _o , s/d _o , d/d _o	4	0.502	57.30	73.47
		6	0.6942	45.10	57.21
		8	0.6805	46.72	58.41
		10	0.7355	43.01	53.07

313

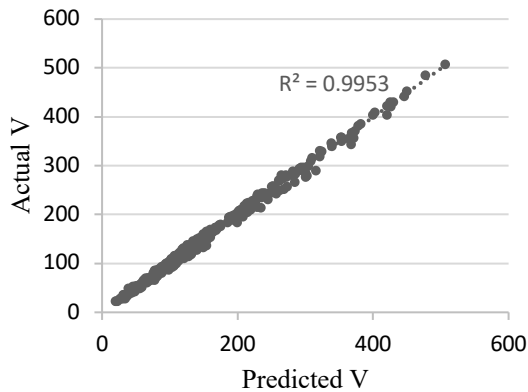


Figure 5: Actual vs Predicted shear buckling Model 1 with 4 Neurons

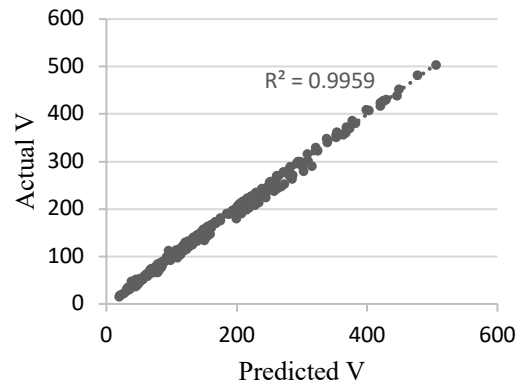


Figure 6: Actual vs Predicted shear buckling Model 2 with 4 Neurons

314

In order to further validate the obtained results, the impact of inputs was assessed using the

315

connection weight approach explained in Section 4.3. Figure 7 provides the impact that each

316

input parameter within the ANN model has on the shear resistance outputs for the different

317

neural network setups. When reviewing model 1 and 2, it can be seen that there is a

318

consistency in the impact of each geometric input parameter for all neural networks analysed.

319

The results further validate the ANN model as it shows that the input parameters that have

320 positive impact on strength are s , H and t_w . This agrees with what would have been expected,
321 as increasing these parameters leads to an increase in shear strength. The input parameters
322 that have a negative impact on strength is d_o . This once again agrees with what is expectable,
323 as increasing this parameter results in a decrease in strength. Although model 3 shows some
324 form of consistency in the impact of inputs, model 4 showed no level of consistency. Based
325 on the results obtained it can be concluded that geometric ratios as inputs, used for models 3
326 and 4 are not effective parameters to predict the shear resistance of web-post using the ANN.
327 The low statistical accuracy that can be noted in Table 6 is reflected in the irregular
328 consistency that can be noted in Figure 7 c) and d). As noted previously, these results do not
329 correlate to the accuracy of the ANN model therefore the potential of an ill function. The
330 results simply provide another form of validation for the Models 1 and 2, in which the input
331 parameters are impacting the output variable as would be expected. In conclusion, since
332 Models 1 and 2 provide predictions with high level of accuracy and the impact of the inputs
333 on the shear strength is as theoretically expected, they are used in the following sections.

334

335

336

337

338

339

340

341

342

343

344

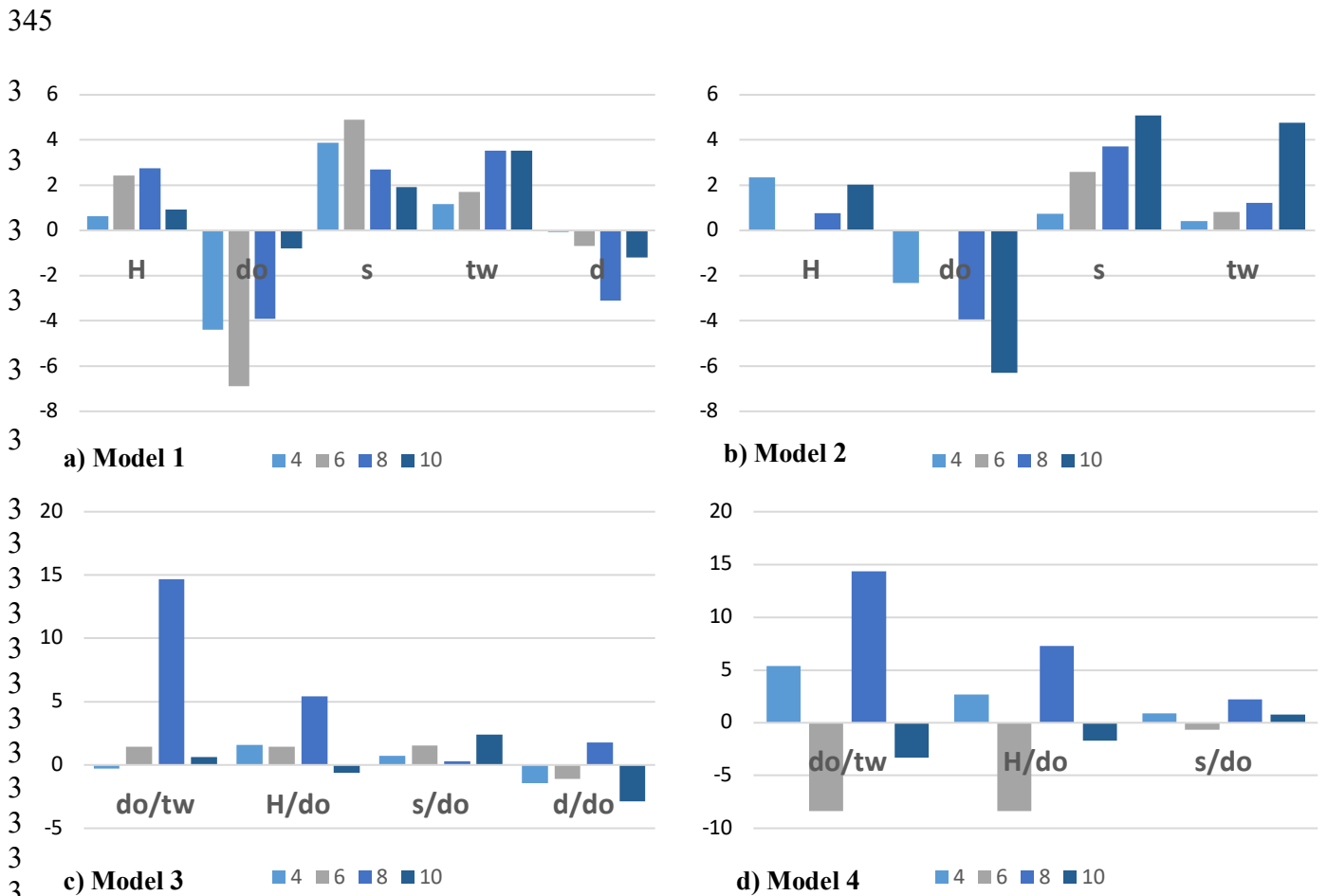


Figure 7: Impact of input parameter on WPB shear resistance

5.2 Comparison to existing analytical models

Table 7 illustrates statistics comparison between the shear resistance of the web-post results predicted by FE models with those predicted by design guidance for cellular beams given in SCI P355 [10] and more recent analytical model proposed by Shamass and Guarracino [11]. The FE results are also compared with those predicted by ANN Model 1 and Model 2 with 4 and 10 neurons. It is worth mentioning that in the analytical model proposed by Shamass and Guarracino [11], the boundary condition coefficient was assumed to be no less than 0.3 and the width of the ideal strut was taken no more than $0.5s_o$.

From the Table 7, it can be noted that the ANN Model 1 with 4 and 10 neurons and Model 2 with 4 and 10 neurons overestimate the shear buckling results by up to 23.9% ,11.1%, 18.5%

379 and 8.7%, respectively, while the design guidance SCI P355 [10] and Shamass and
380 Guarracino [11] analytical model overestimates the shear buckling by up to 21.4% and 29%,
381 respectively. For other cellular beams, the ANN Model 1 with 4 and 10 neurons and Model 2
382 with 4 and 10 neurons underestimate the shear buckling results by up to 14.8% ,11.9%,
383 19.5% and 13%, respectively, while the design guidance SCI P355 [10] and Shamass and
384 Guarracino [11] analytical model underestimates the shear buckling by up to 30.4% and 40%,
385 respectively. This is not surprising, given that the intrinsic regression provided by ANN,
386 which naturally smooths the deviations which can be shown, on the contrary, by the other
387 models.

388 It can be pointed out that the RMSE values for the shear resistance predicted by the ANN
389 models range between 2.76 and 7.07 while it is 23.76 and 22.23 for the shear resistance
390 predicted by the design guidance SCI P355 [10] and Shamass and Guarracino [11] analytical
391 model, respectively. Thus, the RMSE values for the predicted shear resistance by ANN are
392 much lower than those for the predicted shear resistance by the design guidance [10] and the
393 analytical model [11]. It should be mentioned that Shamass and Guarracino [11] compared
394 their analytical model and SCI P355 [10] predictions with the finite-element predictions for
395 normal and high strength steel. The finite-element element predictions were obtained from
396 the full beam models. Based on their results, the RMSE for the shear strength results
397 predicted by their analytical model and the design guide SCI P355 [10] were 18.5 and 29.3,
398 respectively, for normal strength steel. It was evident that their formulation provided shear
399 buckling results that were in much more agreement with FE results than those predicted by
400 SCI P355 [10].

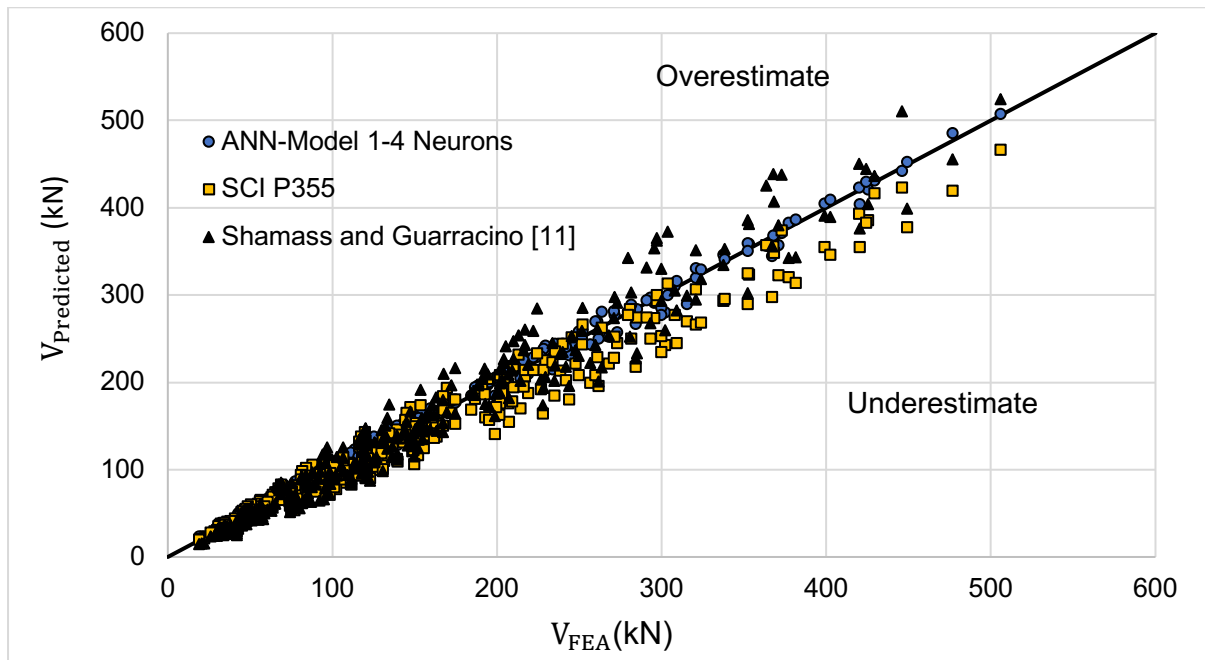
401 Based on the regression values R^2 , it can be observed that ANN models provide the most
402 accurate predictions. Figures 8(a) and 8(b) show a graphical representation of ANN Model 1
403 and 2 with 4 neurons, the design guidance [10] and the analytical model [11] predictions

404 together with the FE predictions. Overall, the ANN model tends to provide the most accurate
 405 shear resistance predictions while the analytical models tend to underestimate the predicted
 406 web-post shear resistance of cellular beams.

407 Table 7: comparison between FEA shear buckling results with analytical and ANN predictions

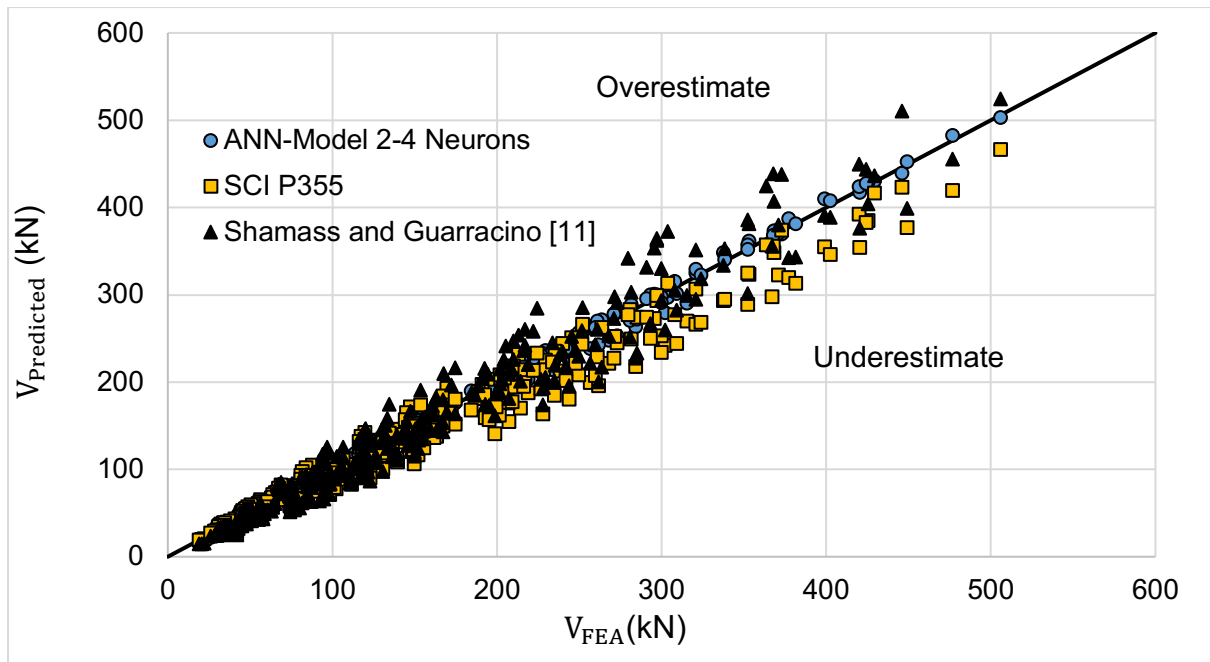
	Model 1- 4 neurons	Model 1- 10 neurons	Model 2- 4 neurons	Model 2- 10 neurons	SCI P300 [10]	Shamass and Guarracino [11]
Maximum percentage difference (%)	23.9	11.0	18.5	8.7	21.4	29
Minimum percentage difference (%)	-14.8	-11.9	-19.5	-13.0	-30.4	-40
R ²	0.995	0.999	0.996	0.999	0.981	0.986
RMSE	7.07	3.36	6.67	2.76	23.76	22.23

408
 409
 410



411
 412
 413
 414

(a)



(b)

Figure 8: Comparison of the predicted shear strength with the FE shear strength

4.2 Comparison with experimental results

Equation 5 shows that as the number of hidden neurons increases, more terms are expected to determine the normalised output value of the shear strength. It can be seen from the Table 7 that ANN Model 1 with 4 neurons provides accurate shear strength predictions and the ANN-based formula to predict normalised shear resistance $(V)_n$ is shown in the Equation 11. In order for engineers to use this equation, the cellular beams geometric parameters H , d_o , s and t_w would have to fall within the X_{min} and X_{max} range stated in Table 3. These parameters will then need to be normalised using Equation 4 and used in Equation 12. Hence, $(H)_n$, $(d_o)_n$, $(s)_n$, and $(t_w)_n$ are the normalised values of the height, opening diameter, opening spacing and web thickness, respectively. Thereafter, in order to determine the shear strength of the web-post (V) from normalised values of the shear strength $((V)_n)$, Equation 4 will need to be used. Table 8 illustrates comparison between web-post shear resistances observed experimentally by Grilo et al. [4] and Tsavdaridis and D’Mello [5] with those predicted by ANN-based

436 formula, design guidance SCI P355 [10] and finite element (FE) results. It can be seen that
 437 ANN provides good web-post shear resistance predictions with RMSE of 19.7 and MAE of
 438 16.5. ANN-based formula generally provides conservative predictions in comparison with the
 439 test results. The reason is due to the fact that the FE web-post shear resistance results used to
 440 train and validate the ANN models are obtained for mild steel with yield stress of 355 Mpa
 441 while the actual values yield stress of the experimentally tested cellular beams range from
 442 375.5 Mpa to 449 Mpa. If we assume that there is a linear relationship between shear strength
 443 of web-post of cellular beams and the yield stress of normal strength steel, the ANN
 444 predictions can be multiplied by the factor of $355/f_{y(\text{tested})}$. The updated shear strength results
 445 predicted using ANN-based formula are shown in the Table 8 and it can be seen that further
 446 improvement of the results is obtained.

447 It can be pointed out that the RMSE and MAE values for the shear resistance predicted by the
 448 ANN-based formula are lower than those obtained for the shear resistance predicted by the
 449 design guidance SCI P355 [10]. Based on the regression values R^2 , it can be observed that
 450 ANN-based formula predicts results more in-line with test results than those obtained by SCI
 451 P355 design guidance. Figures 9 shows a graphical representation of ANN-based formula,
 452 SCI P355 and FE shear strength predictions together with the experimental predictions. It can
 453 be noted that the ANN predictions are in-line with FE predictions.

454

$$(V)_n = -0.1 - 0.23 \frac{2}{(1 + e^{(-2H_1)}) - 1} + 1.22 \frac{2}{(1 + e^{(-2H_2)}) - 1} + 3.69 \frac{2}{(1 + e^{(-2H_3)}) - 1} - 1.53 \frac{2}{(1 + e^{(-2H_4)}) - 1} \quad (11)$$

455

456 Where:

$$\begin{aligned} H_1 &= 1.89 + 1.92(H)_n - 1.86(d_o)_n + 2.6(s)_n - 0.9(t_w)_n \\ H_2 &= 0.91 + 0.6(H)_n - 1.55(d_o)_n + 2.32(s)_n - 0.93(t_w)_n \\ H_3 &= -0.77 - 0.21(H)_n - 0.55(d_o)_n + 0.36(s)_n + 0.55(t_w)_n \\ H_4 &= -1.64 - 1.86(H)_n - 0.75(d_o)_n + 1.84(s)_n + 0.42(t_w)_n \end{aligned} \quad (12)$$

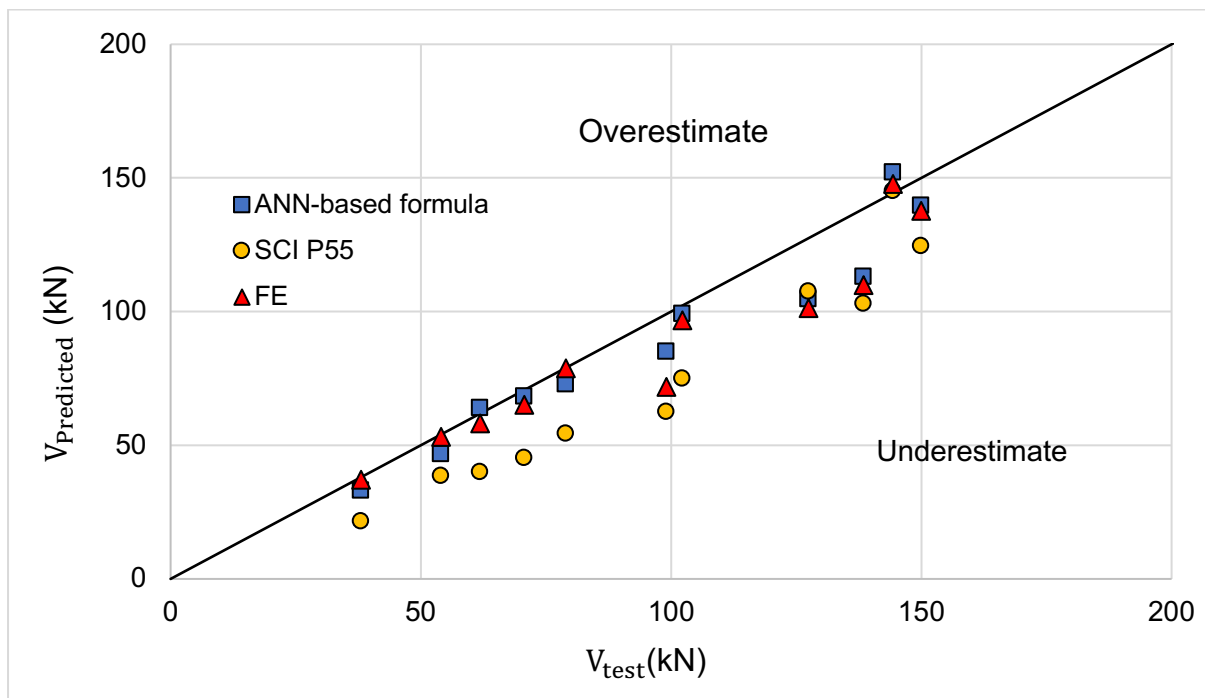
457

458
459

Table 8: Comparison with experimental results

Spec.	V_{test} (kN)	Percentage difference (%)			
		V_{ANN}	$(355/f_{y(tested)})V_{ANN}$	SCI P355	FE
A1	38	-31.4	-13.3	-43.2	-2.3
A2	61.9	-11.8	3.4	-35.1	-6.0
A3	70.7	-13.5	-3.3	-36.0	-7.8
A5	99.1	-26.8	-14.2	-36.8	-27.4
A6	102.2	-13.3	-3.0	-26.6	-5.4
B1	54	-22.8	-13.5	-28.6	-1.6
B2	79	-10.4	-7.8	-31.1	-0.2
B5	138.5	-27.2	-18.4	-25.6	-20.6
B6	150	-17.0	-6.9	-16.9	-8.2
C1	144.4	-0.4	5.3	0.5	2.3
C2	127.5	-22.3	-17.8	-15.7	-20.5
R^2		0.949	0.983	0.911	0.974
RMSE		19.7	12.3	24.5	15.0
MAE		16.5	9.7	22.6	10.4

460



461

Figure 9: Comparison of the predicted shear strength with the experimental shear strength

462
463

464

465

466 **6. Concluding Remarks**

467 The aim of this study is to predict the vertical shear strength of cellular beams made from
468 normal strength steel S355 using ANN and to propose an ANN-based formula to accurately
469 compute the web-post buckling strength of cellular beams, as a function of independent
470 geometrical parameters. Based on analysis and results obtained, it can be concluded that:

- 471 • Out of the 4 different ANN models produced, the models relying on the input of
472 geometric parameters provided a much greater level of accuracy than models based
473 on geometric ratios only. Results showed that the most accurate results were obtained
474 for ANN model 2 which consisted of H , d_o , t_w , s as the input parameters.
- 475 • The general trend for each model was that as the number of neurons increased in the
476 hidden layer, the level of accuracy increased, too.
- 477 • When reviewing the impact of inputs in each of the models, the ANN models based
478 on geometric parameters were further validated as the impact correlates with what is
479 expected to occur.
- 480 • ANN model 1 and 2 had a lower RMSE, lower MAE and higher regression for the
481 predicted web-post shear resistance when compared to the design guidance SCI P355
482 [10] and the analytical model [11], leading to higher level of accuracy
- 483 • When compared to experimental data, ANN-based formula provided good predictions
484 of the web-post shear buckling with regression value of 0.949. A greater level of
485 accuracy can be obtained between experimental and ANN predictions if the actual
486 yield stress of the cellular beam is taken into consideration. Additionally, the ANN-
487 based formula provides results that are more in-line with test results that those
488 predicted by SCI P355 design guidance.
- 489 • On account of the high accuracy shown by the ANN-based formula, it can constitute a
490 potential tool for structural engineers who aim to accurately estimate the web-post

491 buckling of cellular steel beams without the use of costly resources associated with
492 FE analysis. This formula can be easily implemented in Excel or in user graphical
493 interface.

494

495 **Acknowledgment**

496 The authors would like to acknowledge the Centre for Civil and Building Services
497 Engineering at London South Bank University for the encouragement and providing technical
498 supports for this research. Furthermore, they would also like to acknowledge the assistance of
499 our postgraduate student Elida Ceka for her assistance in the parametric study of the FE
500 analysis.

501

502

503

504

505

506

507

508

509

510

511

512

513

514

515

516 **References**

- 517 [1] Mesquita, L.M.R., Gonçalves, J., Gonçalves, G., Piloto, P.A.G. and Kada, A. (2015). Intumescent
518 fire protection of cellular beams. In *X Congresso de Construção Metálica e Mista* (pp. 623-630). CMM-
519 Associação Portuguesa de Construção Metálica e Mista.
520
- 521 [2] Fares, S. S., Coulson, J. & Dinehart, D. W. (2016). Castellated and Cellular, Beam Design. *American*
522 *Institute Of Steel Construction - Steel Guide*.
523
- 524 [3] Aglan, A.A. and Redwood, R.G., (1974). WEB BUCKLING IN CASTELLATED
525 BEAMS. *Proceedings of the Institution of Civil Engineers*, 57(2), pp.307-320.
526
- 527 [4] Grilo, L.F.; Fakury, R.H. and de Souza Veríssimo, G. (2018). Design procedure for the web-post
528 buckling of steel cellular beams. *Journal of Constructional Steel Research*, 148, pp.525-541.
529
- 530 [5] Tsavdaridis, K.D. and D'Mello, C. (2011). Web buckling study of the behaviour and strength of
531 perforated steel beams with different novel web opening shapes. *Journal of Constructional Steel*
532 *Research*, 67(10), pp.1605-1620.
533
- 534 [6] Erdal, F. and Saka, M.P. (2013). Ultimate load carrying capacity of optimally designed steel cellular
535 beams. *Journal of constructional steel research*, 80, 355-368.
536
- 537 [7] Panedpojaman, P.; Thepchatri, T. and Limkatanyu, S. (2014). *Novel design equations for shear*
538 *strength of local web-post buckling in cellular beams*. *Thin-walled structures*, 76, pp.92-104.
539
- 540 [8] Ward, J. (1990). Design of Composite and Non-Composite Cellular Beams, 100, The Steel
541 Construction Institute, SCI Publication.
542
- 543 [9] Lawson, R.M., Lim, J., Hicks, S.J. and Simms, W.I. (2006). *Design of composite asymmetric*
544 *cellular beams and beams with large web openings*. *Journal of Constructional Steel Research*, 62(6),
545 pp.614-629.
- 546 [10] Lawson, R.M. and Hicks, S.J. (2011). Design of composite beams with large web openings–SCI-
547 P-355. *The Steel Construction Institute: Ascot*.
548
- 549 [11] Shamass, R. and Guarracino, F. (2020). Numerical and analytical analyses of high-strength steel
550 cellular beams: A discerning approach. *Journal of Constructional Steel Research*, 166, p.105911.
551
- 552 [12] Shamass, R. Alfano, G. and Guarracino, F. (2014). A numerical investigation into the plastic
553 buckling paradox for circular cylindrical shells under axial compression. *Engineering Structures*, 75,
554 pp.429-447.
555
- 556 [13] Shamass, R. Alfano, G. and Guarracino, F. (2015). An analytical insight into the buckling paradox
557 for circular cylindrical shells under axial and lateral loading. *Mathematical Problems in Engineering*,
558 Article number 514267, doi: 10.1155/2015/514267, pp. 1-11.
559
- 560 [14] Shamass, R. Alfano, G. and Guarracino, F. (2015). An investigation into the plastic buckling
561 paradox for circular cylindrical shells under non-proportional loading. *Thin-Walled Structures*, 95, , pp.
562 347-362.

563

564 [15] Shamass, R. Alfano, G. and Guarracino, F. (2017). On Elastoplastic Buckling Analysis of
565 Cylinders Under Nonproportional Loading by Differential Quadrature Method. *Int J of Structural*
566 *Stability and Dynamics*, 17 (7), Article number 1750072.

567

568 [16] Ozcan, F., Atis, C., Karahan, O., Uncuoglu, E. and Tanyildizi, H. (2009). Comparison of
569 artificial neural network and fuzzy logic models for prediction of long-term compressive strength of
570 silica fume concrete. *Advances in Engineering Software*, 40 (9), pp.856-863.

571

572 [17] Golafshani, E.M., Rahai, A., Sebt, M.H. and Akbarpour, H. (2012). Prediction of bond strength
573 of spliced steel bars in concrete using artificial neural network and fuzzy logic. *Construction and*
574 *Building Materials*, 36, pp.411-418.

575

576 [18] Kamane, S.K., Patil, N.K. and Patagundi, B.R. (2020). Use of artificial neural networks to Predict
577 the Bending Behaviour of Steel I Beam Externally attached with FRP Sheets. *Materials Today:*
578 *Proceedings*, (in press)

579

580 [19] Tran, V., Thai, D. and Nguyen, D. (2020). Practical artificial neural network tool for predicting the
581 axial compression capacity of circular concrete-filled steel tube columns with ultra-high-strength
582 concrete. *Thin-Walled Structures*, 151, 106720.

583

584 [20] Hedayat, A.A., Afzadi, E.A., Kalantaripour, H., Morshedi, E. and Iranpour, A. (2019). A new
585 predictive model for the minimum strength requirement of steel moment frames using artificial neural
586 network. *Soil dynamics and Earthquake Engineering*, 116, pp.69-81.

587

588 [21] Hedayat, A., Jazebu, E., AsadAbadi, S. and Iranpour, A. (2018). Flexural Strength Prediction of
589 Welded Flange Plate Connections Based on Slenderness Ratios of Beam Elements Using ANN.
590 *Advances in Civil Engineering*, 2018, 8059190.

591

592 [22] Pu, Y. and Mesbahi, E. (2006). Application of artificial neural networks to evaluation of ultimate
593 strength of steel panels. *Engineering Structures*, 28 (8), pp.1190-1196.

594

595 [23] Hosseinpour, M., Sharifi, Y. and Sharifi, H. (2020). Neural network application for distortional
596 buckling capacity assessment of castellated steel beams. *Structures*, 27, pp.1174-1183.

597

598 [24] Tohidi, S. and Sharifi, Y. (2014) Inelastic lateral-torsional buckling capacity of corroded web
599 opening steel beams using artificial neural networks. *The IES Journal Part A: Civil & Structural*
600 *Engineering*, 8, pp. 24-40.

601

602 [25] Sharifi, Y., Moghbeli, A., Hosseinpour, M. and Sharifi, H. (2019). Study of neural network
603 models for the ultimate capacities of cellular steel beams. *Iranian Journal and Science and*
604 *Technology, Transactions of Civil Engineering*, 44, pp.579-589.

605

606 [26] Sharifi, Y., Moghbeli, A., Hosseinpour, M. and Sharifi, H. (2019). Neural networks for lateral
607 torsional buckling strength assessment of cellular steel I-beams. *Advances in Structural Engineering*,
608 22(3), 136943321983617

609

610 [27] Abambres, M., Rajana, K., Tsavdaridis, K.M. and Ribeiro, T.P. (2018). Neural network-based
611 formula for the buckling load prediction of I-section cellular steel beams. *Computers*, 8(1), pp.1-26.
612

613 [28] Nguyen, Q.H., Ly, H., Le, T. and Nguyen, T. (2020). Parametric Investigation of Particle Swarm
614 Optimization to Improve the Performance of the Adaptive Neuro-Fuzzy Inference System in
615 Determining the Buckling Capacity of Circular Opening Steel Beams. *Materials*, 13(10), 2210.
616

617 [29] Gholizaadeh, S., Pirmoz, A. and Attarnejab, R. (2011). Assessment of load carrying capacity of
618 castellated steel beams by neural networks, *Journal of Construction Steel Research*, 67 (5), pp.770-
619 779.
620

621 [30] MATLAB and Statistics Toolbox Release 2019a, The MathWorks, Inc., Natick, Massachusetts,
622 United States.
623

624 [31] Golafshani, E. M., Rahai, A., Sebt, M. H. and Akbarpour, H. (2012) Prediction of bond strength
625 of spliced steel bars in concrete using artificial neural network and fuzzy logic, *Construction and*
626 *Building Materials*, 36 , p. 411-418.
627

628 [32] Gupta, T., Patel, K. A., Siddique, S., Sharma, R. K. and Chaudhary, S. (2019) Prediction of
629 mechanical properties of rubberised concrete exposed to elevated temperature using
630 ANN, *Measurement*, 147 , p. 106870.
631

632 [33] Olden, J. D., Joy, M. K. and Death, R. G. (2004) An accurate comparison of methods for
633 quantifying variable importance in artificial neural networks using simulated data, *Ecological*
634 *Modelling*, 178 (3), pp. 389-397.
635
636